

Damage growth in fused silica optics at 351 nm: refined modeling of large-beam experiments

L. Lamaignère · G. Dupuy · A. Bourgeade ·
A. Benoist · A. Roques · R. Courchinoux

Received: 5 February 2013 / Accepted: 13 June 2013 / Published online: 10 July 2013
© The Author(s) 2013. This article is published with open access at Springerlink.com

Abstract Up to now, laser damage growth on the exit surface of fused silica optics has been mainly considered as exponential, the growth coefficient depending essentially on fluence. From experiments with large beams carried out at 351 nm under nanosecond pulses, a statistical analysis is conducted leading to a refined representation of the growth. The effect of several parameters has been taken into account to describe precisely the growth phenomenon. The two principal parameters proved to be the mean fluence and the size of the damage sites. Nevertheless, contributions of other parameters have been estimated too: the number of neighbors around the damage site, the shot number, etc. From experimental results, a model smoothed on a statistical approach is developed that permits the description of a complete sequence of growth. To evaluate the relevance of the modeling approach, the occluded area estimated from modeling is compared with the ones experimentally measured. For this purpose, numerical growth methods have been developed too. It is shown that the approach outlined is appropriate for a more precise description of the growth.

1 Introduction

Laser damage sites are weak areas for laser-induced damage growth due to their morphologies [1]—microstructure, cracks, compaction layer, point defects and local chemistry—which locally enhance the laser absorption. The development of large aperture and high-power lasers such

as the National Ignition Facility (NIF) and the Laser Megajoule (LMJ) requires the study of the laser damage growth at the surface of fused silica optics [2]. First studies realized with spatially Gaussian small beams (millimeter sized) showed the growth generality (at 1ω and 3ω) and behaviors much more pronounced in the rear face than in the front one. Indeed, front surface growth rate is limited and characterized by a linear growth shot after shot [3]. Observations on the Beamlet laser and the first experimentations on the OSL facility at Livermore [4] revealed the fundamental aspect from an operational point of view: the exponential nature of the growth shot after shot for exit surface damage. This behavior is observed for many sites, but depending on the morphology, some damage sites do not evolve and remain stable up to large fluence. The exponential growth concerns mainly the deep craters (few micrometers), wide (few tens of micrometer) created at high fluences. The exponential feature tends to represent it by a growth rate coefficient given by the following logarithmic ratio:

$$k = \ln \left(\frac{A_{n+1}}{A_n} \right) \quad (1)$$

where A_n and A_{n+1} are, respectively, the areas of the damage site before and after the growth. Then a sequence of N shots leads to an area increase in a factor e^{Nk} [5]. Numerous experimental results obtained by Norton et al. at Livermore are now available. For a long time, they were the nub of the damage growth. Recent publications have made more acute the knowledge of the growth. Let us recapitulate the main points that will help the comprehension of this paper; these remarks are given for the wavelengths of 351 and 355 nm (or 3ω): The average growth rate coefficient is fluence dependent, and it varies linearly with fluence as follows:

L. Lamaignère (✉) · G. Dupuy · A. Bourgeade · A. Benoist ·
A. Roques · R. Courchinoux
CEA-CESTA, 15 Avenue des Sablières, CS 60001,
33116 Le Barp Cedex, France
e-mail: laurent.lamaignere@cea.fr

$$\langle k \rangle = C(F - F_{\text{th}}) \quad (2)$$

where F_{th} is the fluence threshold for growth (in J/cm^2). It means that below this threshold, damage sites do not evolve and remain stable; above this threshold, damage sites grow more and more rapidly with fluence. C represents the rate of increase (in cm^2/J). This standard approach of the growth is referred as the linear model in this paper. Recent papers showed that these two coefficients depend slightly on pulse duration [6]. Up to a recent study, the growth phenomena were considered as independent of the damage size, meaning that the growth coefficients are the same whatever the sizes and the morphologies of damage sites. In a clever approach, Negres et al. [7] pointed out the effects of current size on growth for sites with diameters in the range of 50–1,000 μm , which is well described in terms of Weibull statistics. This approach is innovative and gives a new insight on the growth phenomenology. More recently, Negres et al. [8] demonstrated that the onset of damage growth depends both on the current size of a damage site and on the laser fluence to which it is exposed, highlighting that damage growth is probabilistic for small damage sites (in the range 7–50 μm). For a better comprehension of the growth mechanisms, let us describe first the damage morphology once a damage site is initiated with a first laser irradiation. Wong et al. [1] observed two different regions: a central “core” located at the bottom of the damage crater characterized by a highly scattering, modified and densified material with numerous light-absorbing defects and numerous cracks located below this layer; the edges of this crater are cleaved surfaces of mechanically damaged material with cracks that radiate toward the surface. By means of a time-resolved microscope system, Demos et al. [9] studied the dynamics of energy deposition and the subsequent crack propagation. This study reveals that the energy deposition takes place in the central “core” region and at the intersection of the cleaved surface of the damage site with the surface of the optic. More and more plasmas are formed with increasing fluence, and they can merge to cover the core region. The presence of defects in this region initiates an increase in the conduction band electron population [10]. The circumferential and radial cracks formed during damage growth are then due to stresses developed by the pressure pulse following the laser energy deposition. The plasma is formed before the peak of the pump pulse, and then for shorter pulses, the energy deposition process is shortened, and then the length of cracks formed is reduced. At the opposite, for longer pulses the amount of cracks and their size increase leading to a rate increase by which the damage site grows characterized by the exponential growth reported in literature [6]. From these observations, the exponential growth behavior is deeply linked to the size of the “core” region

and the space with the cracks on the edges; in other words, the damage size has to be considered. Other considerations have also to be taken into account: Two close damage sites will merge forming a new damage site with a different morphology and then a different growth rate; the shot sequence is another parameter that contributes to different growth rates and/or behaviors; a conditioning effect could be observed or in the other hand a fatigue effect. All these points contribute to make more acute the exponential law in light of these considerations. The issue of front surface damage growth is different: The morphology of damage site to the front face is usually minimal as any ejected material vaporizes in the form of plasma and it absorbs the incoming radiation. In consequence of this, rear surface damage is usually more catastrophic than front surface damage. On the front face, the plasma shields from the incoming light and only a weak shock wave are launched into the substrate: The front surface is weakly damaged. Moreover, an optical component illuminated by a collimated beam will usually damage at the exit surface at a lower fluence than at the entrance surface. No front surface damage sites being initiated during experiments, front damage growth is not considered.

In this paper, we report growth experiments that have been performed with centimeter-sized beams. The use of large beams permits first the observation of the growth up to large damage area, secondly the study of numerous damage sites at the same time allowing the development of a statistical approach to describe this phenomenon. The results complete previous observations of Negres et al. [7, 8] and above all permit us to propose a new approach to describe the growth leading to a revisited growth law. The model that has been developed takes into account several parameters: the damage sizes, the local fluences, the shot number (background history of the shot sequence), the number of neighbors (damage sites close to the studied site), the optics thickness and the phase modulations. The influence of each parameter has been evaluated separately. This model will be referred in the following as the multi-parameter model. To check the validity of the modeling, we have chosen to compare the occluded areas, measured during the experiments shot after shot and estimated from the modeling. This work has been first realized on subaperture areas in order to correctly measure growth coefficients of isolated damage sites that did not merge. After that, the comparison between experiment and modeling has been realized on the full aperture of the beam. In the modeling part, several numerical growth methods have been tested and qualified too. The choice of the numerical method can affect more or less the final estimation of the occluded area. In Sect. 2 of this paper, we describe how tests are carried out. Section 3 is devoted to experimental results. The modeling part is given in Sect. 4. The

comparison between experiments and modeling is discussed in Sect. 5. It is shown that the estimation of the occluded area at the end of the growth run is well comparable to the real occluded area experimentally measured. This approach provides a straightforward means of predicting the growth of an optics illuminated with large and inhomogeneous beams: The two main parameters that have to be precisely measured are the local fluence on the damage and its size.

2 Materials and methods

2.1 Test facility

The growth study requires large and energetic beams. Experiments have been performed with a Nd: glass laser facility that can produce 0.5- to 20-ns laser pulses >200 J at 1,053 nm (ALISÉ facility). Frequency conversion is realized on the laser damage test bench (see Fig. 1) by means of two type-II KDP crystals: Energies up to 50 J at 351 nm are delivered. The beam on the sample is reduced with a 3-m focal lens to obtain sufficiently high fluences. Tests are realized at intermediate plane, and the beam diameter is about 16 mm (see Fig. 2). For this work, 3-ns

flat-in-time pulses with a high front rise have been used (See Fig. 3 of Ref. [11]). The repetition rate was a shot per hour to allow the thermal decay of the glass amplifiers. For each shot, different phase modulation of the beam could be enabled/disabled: at 2 GHz to suppress stimulated Brillouin scattering (SBS) and at 14 GHz for beam smoothing by spectral dispersion. In case of thick optical components, 2 GHz is compulsory to avoid the front surface damage of the optic due to the backward-propagating SBS (BSBS) [11]. As those phase modulations will be used on LMJ beams, the experiments and measurements made are fully representative of LMJ's operational conditions when the modulations are enabled. The characteristics of this laser are quite similar to high-power lasers such as LMJ and NIF; let us mention the front-end, the amplification stage, the spatial filters and the frequency converter crystals. Then laser damage measurements taken with this system should be representative of the damage phenomenon on high-power lasers. The metrology is very close to small beam metrology [12]: Energy, temporal and spatial profiles are recorded. For the latest, a charge-coupled device (CCD) camera is positioned at a plane optically equivalent to that of the sample (the main characteristics of the laser and measurement principles are reported in Ref. [13]). CCD pixel resolution (taking into account magnification on the

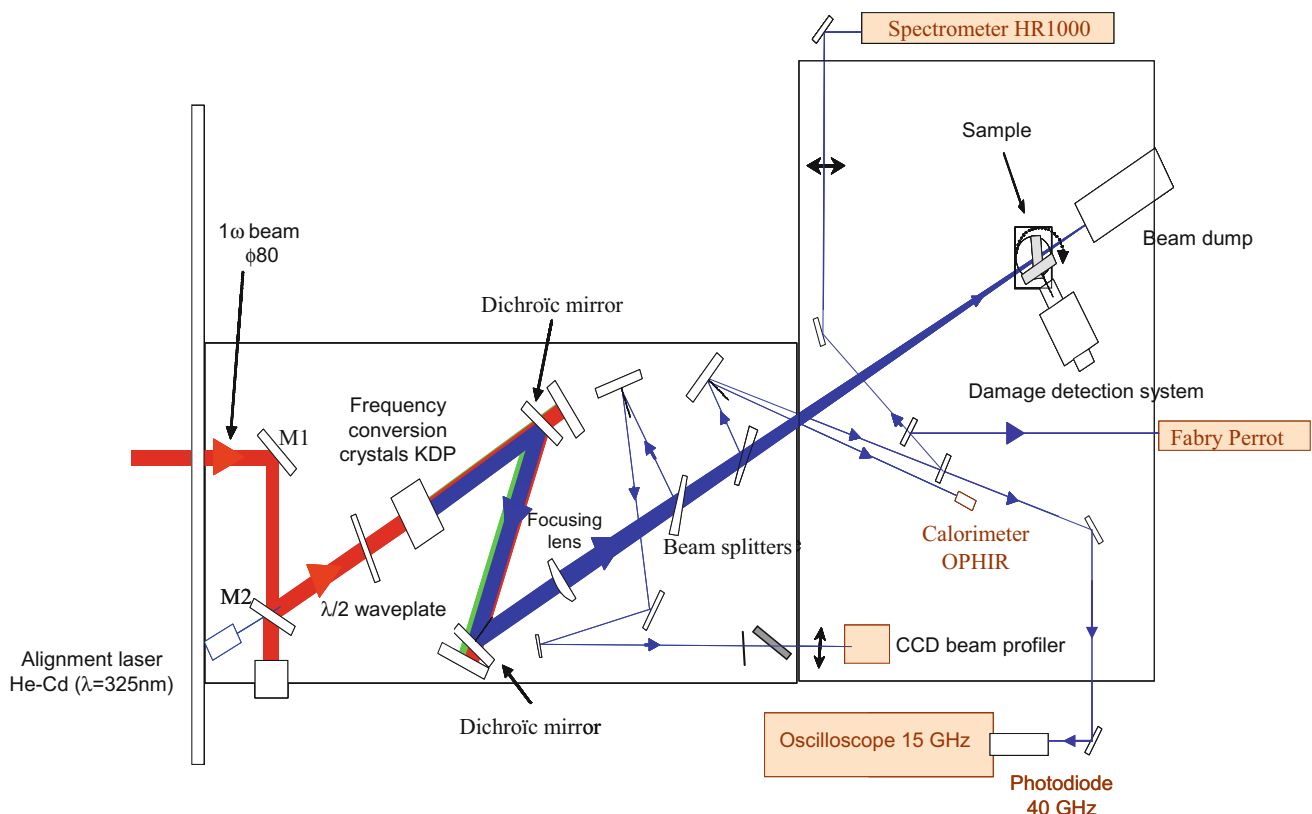


Fig. 1 Experimental setup

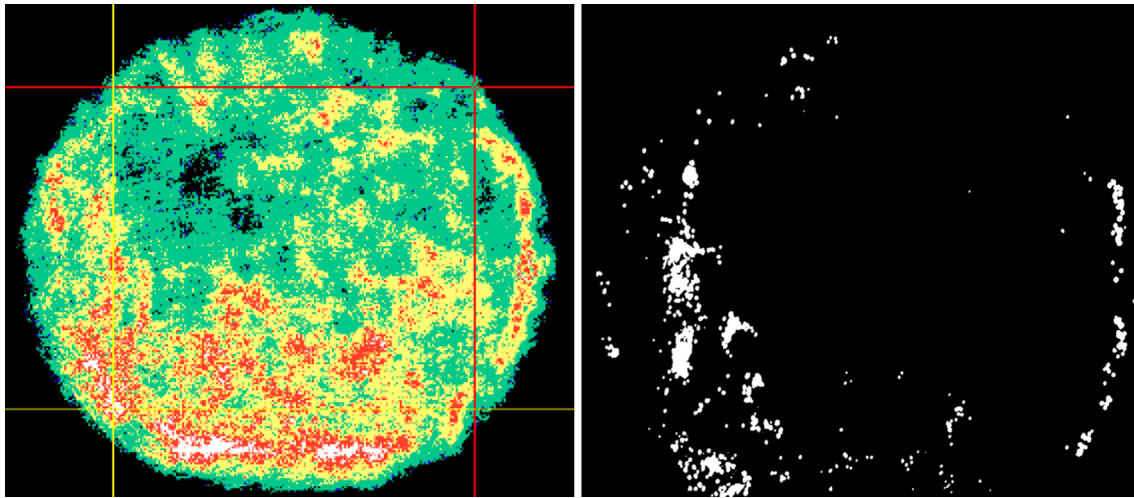
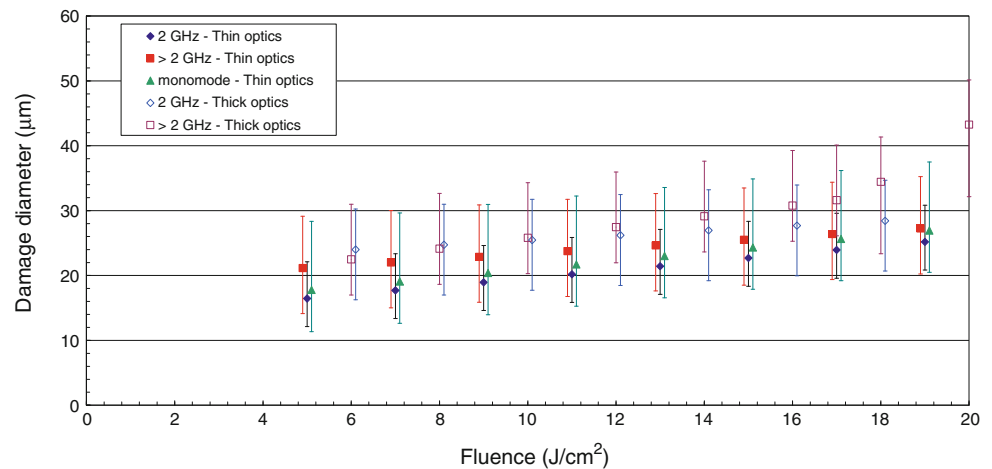


Fig. 2 Damage test with a centimeter-sized beam. On the *left*, spatial profile of the 16-mm-diameter beam at the sample plane as measured on CCD camera. The beam contrast is about 38 %. On the *right*, the

corresponding damage photography is reported. Matching the two maps allows us to extract the fluence for each damage site

Fig. 3 Damage diameter as a function of fluence, for several phase modulations and thin or thick optics. *Error bars* represent the standard deviation for a given configuration. Experimental results are the mean of three shots in the same conditions



CCD) is $22 \times 22 \mu\text{m}^2$. Beam profile and absolute energy measurement give access to energy density $F_{(x,y)}$ locally in the beam:

$$F_{(x,y)} = \frac{E_{\text{tot}}}{S_{\text{pix}} \times \sum_{x=\min}^{x=\max} \sum_{y=\min}^{y=\max} i_{(x,y)}} \times i_{(x,y)} \quad (3)$$

E_{tot} total energy; S_{pix} CCD pixel area; $i_{(x,y)}$ pixel gray level.

Due to a contrast inside the beam itself (peak to average) of about 4, a shot at a given average fluence covers a large range of local fluences (see Fig. 2). This makes compulsory the exact correlation between local fluence and local damage size and position.

2.2 Samples and test procedure

For this study the laser damage of synthetic fused silica (HEREAUS S312) windows, superpolished by SESO

company, is dealt with. All tested samples were antireflection treated with a sol-gel-based process, as in operational conditions and to limit the SBS effect. One-hundred-millimeter-diameter-size samples have been used: About 12 different sites per sample have been illuminated with several laser experimental configurations, mainly in terms of phase modulations. Sample thicknesses are 10 and 34 mm, the latest being representative of thick component used as LMJ vacuum window of target chamber.

The first step concerns the damage initiation shot: The 16-mm-diameter beam (see Fig. 2a) irradiated a zone where no defect was visible and that had never been irradiated before. Tests are realized at normal incidence. This first illumination leads to the formation of numerous damage sites, distributed as a function of fluence. It means that damage sites were initiated from defects on the exit surface of fused silica optic. For each damage site, the local

peak fluence is known matching fluence and damage map. The damage density $D(F)$ is then determined [11]. At this step, peak intensity is not considered. This latest point is under investigation both from a point of view of local absorption by the defects and in terms of nonlinear propagation through the optic. At the end of this step, damage sizes are also precisely measured. It appears that damage diameters increase linearly and slowly with fluence from 20 to 30 μm (see Fig. 3). In this graph, each point is the mean of three shots; error bars represent the standard deviation for a given configuration. We note that these observations are coherent with the previous results published by Carr et al. [14] in terms of size and behavior. Carr reports diameters close to 15 μm at 3 ns and a fluence dependence too. The precise knowledge of the size of each initiated damage site permits the study of the growth. Next, six additional shots are fired that induced an increase in the damaged areas, new fractures forming and eventually ripping off new material. The sequence is stopped when too many sites coalesce. After each shot, the illuminated area is carefully observed. A digital CCD camera (Nikon D2X) with a 200-mm objective is used. The sample is illuminated by means of white light emission diode (LED) bars through two opposite edges perpendicular to the component. The observation field is about 25 mm \times 20 mm, covering the entire illuminated area. To extract and measure damage areas from images, a binarization threshold is carried out on ImageJ software. The optical resolution is about 5 μm . For the first shot, only few damage sites are initiated. So, each of them has been precisely observed to measure its area with accuracy. This precaution is important to carefully determine the growth coefficients during the first steps where damage sites are small, potentially leading to large uncertainties. Then damage map is next superimposed to fluence map allowing the attribution of peak fluence or mean fluence to each damage site (map superposition is realized by means of reference points in the beam, hot spots). In this procedure, the beam profile image is resized and resampled to fit the corresponding damage site mapping, which is considered as the reference image. The camera's depth of field is sufficiently small to consider only surface damage and not bulk damage in case of self-focusing for thick components. For each shot, the beam profile was recorded to take into account beam changes during experiments.

To recapitulate several parameters of this study, Table 1 runs over the experimental variables adjusted during the whole tests.

3 Experimental results

A clear aperture of $9 \times 9 \text{ mm}^2$ centered on the beam is first considered. That permits to avoid some hot spots

Table 1 Parameters of the experiments and variables adjusted in the multiparameter model and their influence on damage growth prediction

Parameters	Value	Influence
Thickness (mm)	10 or 34	None
Phase modulation (GHz)	2; 14; 2 and 14; none	None
Mean fluence (J/cm^2)	0 to 20	Major
Damage area (μm^2)	10^2 to 10^5	Major
Shot number	1 to 7	Minor
Number of neighbors	1 to 10	Minor

(fluences highest than 30 J/cm^2) on the circumference area, where damage densities are very high, resulting in damage clustering [15]. Few tens of damage sites are tracked during the whole growth sequence. To illustrate growth phenomena, it is reported in Fig. 4 the increase in damage diameters during six shots for each individual damage site. An increase by a decade or more is often observed. Despite the fact that fluences are not reported in this graph (the fluence range extends from 4 to 18 J/cm^2), it appears that growth behaviors are spread out too: Identical damage sites (in terms of apparent size, not morphology) can evolve differently from the others. Some damage growths are well fitted by an exponential law, while others are partly fitted by linear laws. In this figure, a change in the slope in this semilogarithmic representation is perceptible too (dashed areas are just a guide for eye), meaning that other parameters are involved in the description of the growth. It is commonly admitted that the rear growth phenomenon is well characterized by an exponential behavior [4–7] except for shorter pulse duration where a linear growth is sometimes observed [6]. On this basis, we consider the single-shot growth rate coefficient k defined in Eq. (1) [5].

Figure 5 reports the growth coefficients experimentally measured as a function of fluence during a series of six shots, for each individual damage site and after each shot. Results are scattered. For a given fluence, ratio of order 5 is obtained between maximum and minimum values. This dispersion is also observed inside the same shot index. It could be relevant to gather data and to work out the average of inside fluence bins in order to highlight few tendencies. It is then observed (see Fig. 6) that growth coefficients take lower values with increasing shot number up to a steady value. Bold squares represent the experimental averages of all coefficients inside fluence bins. In this graph, the dashed line represents values commonly reported in literature [4]. Bold squares are very close to this line, meaning that the growth behavior can be described in average by a unique value at a given fluence. A growth threshold around 5 J/cm^2 is deduced from this experiment; it corresponds to the threshold previously reported by several authors [4–16]. Shot after shot, damage sites are

Fig. 4 Growth of damage site area versus shot number under laser irradiation at 351 nm—3 ns. In this semilogarithmic representation, the exponential behavior is more often observed. Despite the fact that fluences are not reported in this graph, a precise analysis shows that results are not strictly repeatable. *Dashed areas* are just indicators illustrating a change in the growth behavior

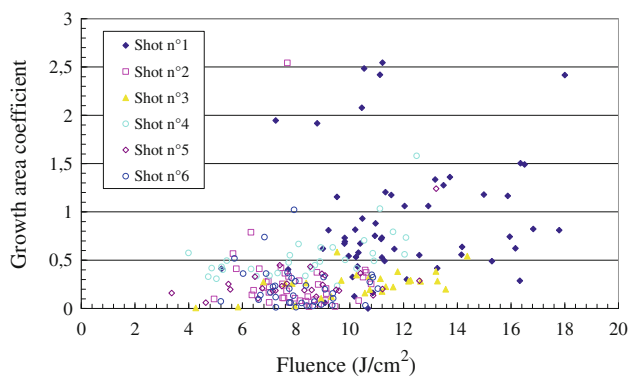
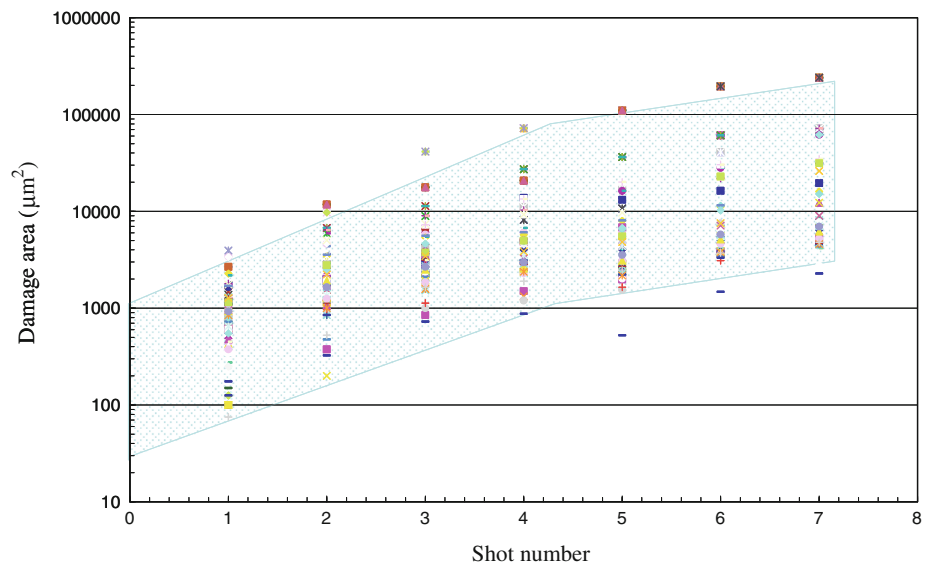


Fig. 5 Growth area coefficient versus fluence and shot number

bigger and bigger, but for a given laser energy deposition, the stresses developed by the pressure pulse remain equal for longer circumferential and radial cracks that are more numerous too. The damage size is then expected to be a relevant parameter to take into account.

In order to explain and justify the growth coefficient decrease shot after shot, we have chosen to represent experimental growth coefficients as a function of damage areas. Results are reported in Fig. 7. A close correlation appears clearly. Higher values are obtained for small damage sites, and a decrease to lower values is observed with larger damage sites. For larger sites, values are lower than 0.5 and tends to a steady value. In this representation, data are less scattered too. Then growth coefficients seem to be dependent nonetheless on fluence but also on size. Figure 8 reports the standard representation of the growth coefficient as a function of fluence where damage sites have also been gathered together in size bins. In this representation, values are very disperse for small damage sites and are more concentrate close to the standard results for

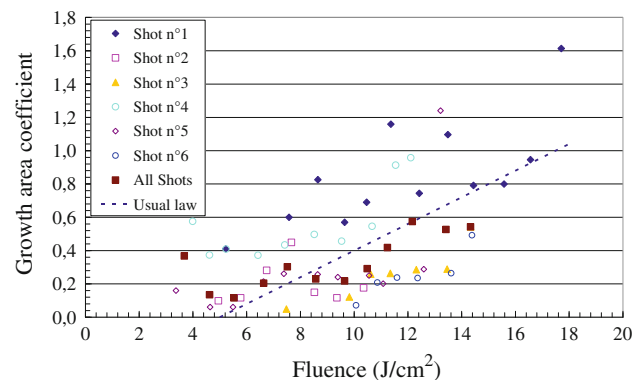


Fig. 6 Mean growth area coefficient versus fluence and shot number

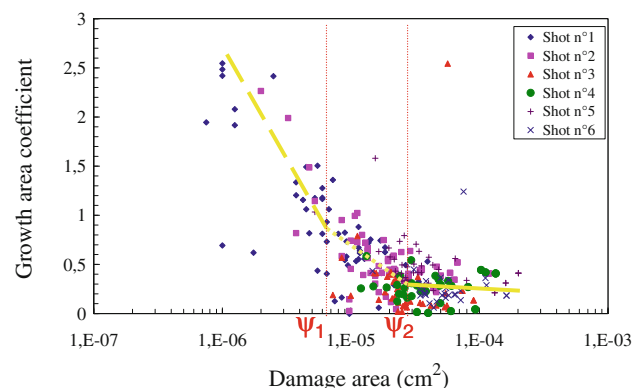
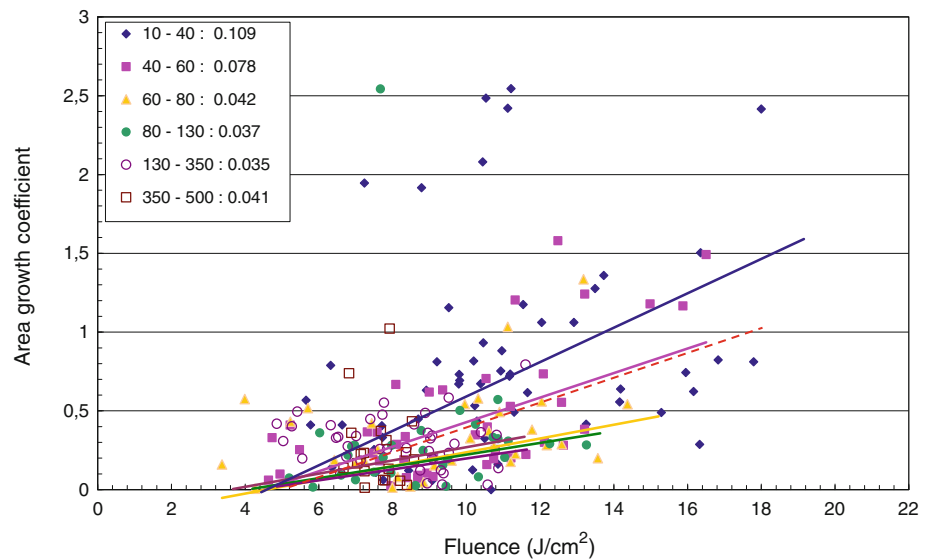


Fig. 7 Growth area coefficient versus damage area and shot number. The *dashed lines* represent the segmented regressions (see text for details)

large damage sites. The average growth coefficients decay with the size of the damage sites. To highlight this, data have been fitted by means of relation (2) for the different size bins (the threshold F_{th} has been fixed close to 4.5 J/

Fig. 8 Growth area coefficient versus fluence and damage size (size bins are expressed in microns). Continuous lines are a fit of experimental data by means of relation (2). Values of the coefficient C are reported in the insert for each size bin. The dashed line is the standard behavior from literature [4–16]



cm^2). The coefficient C of relation (2) is reported in the insert. It decreases as bin size increases up to a steady value close to 0.04.

The whole results go for a more precise description of the growth sequence taking into account the local fluence on the damage site, its size and other parameters identified during the experiments. For instance, it is well known that a ramp of fluence may improve the damage resistance of the optic, and at the opposite, a repeated number of shots may lay to a fatigue effect: The shot sequence is then to consider. The growth phenomenon is mainly characterized by the expansion of cracks which can merge between neighbor sites: The number of neighbors could be a relevant parameter too. A multiparameter model is described in the next paragraph. Modeling results are then compared to experimental ones. Next, the model is applied on the full-aperture beam and again compared to experiments.

4 Multiparameter model

In order to improve the estimate of the single-shot growth rate k defined above, experimental results have been used for a statistical study. We have indeed considered the damage sites and their growth in a zone where the successive laser shots create the less new damage events and where the initial damage sites created by the first laser shot will the less merge.

Growth phenomenology being dependent on fluence and damage area too (see Fig. 7 and Ref. [7]), the model derivation has been led with the mean fluence (F) and the initial damage area (S) as explanatory variables. So, relation (4) has been used to fit experimental growth coefficients:

$$k = \beta_0 + \beta_1 F + \beta_2 S + \varepsilon \quad (4)$$

where β_0 , β_1 and β_2 are adjusting parameters and ε is the part of k which cannot be explained by the estimation. We have then compared growth coefficients obtained with relation (4) to experimental ones. The coefficient of determination was chosen to evaluate the accuracy of the relation. It measures the part of the variance which the model explains. From relation (4), the coefficient was only 0.51: Half of the variance remains random. To improve the quality of the estimation and the modeling, each basic event was then associated with the initial surface of the damage, the maximum, mean and minimum fluences measured on this damage, the laser shot number and the number of other damage sites in a small vicinity of the damage (a radius of 250 μm around the damage site was considered). An analysis of covariance has shown that the maximum and minimum fluences were essentially collinear with the mean fluence. Thus, only the mean fluence has been kept as variable for the analysis. Next, to take into account the nonlinearity of the dependence on the damage surface, we have then used a mixed linear regression. For this we have defined four intervals in order to consider the damage surface as a qualitative variable depending on which interval this surface belonged. The coefficient of determination was then equal to 0.69. Finally, a segmented linear regression has been tested [17]. Three segments were defined for the damage surface variation, and on each segment, the estimation was a linear function of the surface variable (this segmentation is reported in Fig. 7 by means of dashed lines). The coefficient of determination grew then up to 0.75. The final estimation is thus given by:

$$k = \beta_0 + \beta_1 F_{\text{mean}} + \beta_2 S + \beta_3 (S - \psi_1) 1_{S > \psi_1} + \beta_4 (S - \psi_2) 1_{S > \psi_2} + \beta_5 V + \sum_{i=2}^{n_{\text{shot}}} \alpha_i 1_{\text{shot}=i} + \varepsilon \quad (5)$$

To recapitulate, F_{mean} is the mean fluence on the damage site, S is the damage area, ψ_1 and ψ_2 are the values defining the three segments used for the regression, V is the number of neighbors, and α_i is the index shot. On the other hand, we have noticed that the laser shot number and the number of neighbors had a minor influence on the model efficiency. The influence of each parameter is recapitulated in Table 1. Thus, these two variables were not kept in the final model. From this approach, growth coefficients have been estimated for different damage sites, shot after shot during a complete run. Figure 9 compares, for each damage site, the observed growth coefficients with the estimated ones. We notice that the model underestimates the high growth

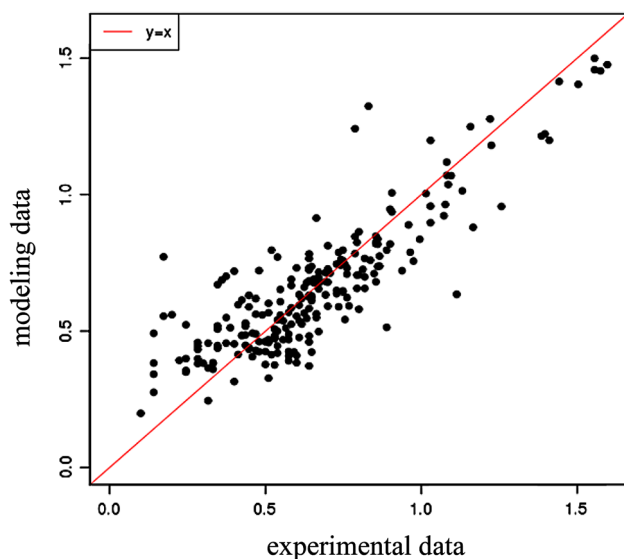


Fig. 9 Growth coefficient: modeling versus experimental data

coefficients and overestimates the small ones; it corresponds to the random part that the model does not describe. Nevertheless, this model has been applied with the estimated growth coefficients in an attempt to reproduce the experimental damage map in the considered area at the end of the seven successive shots. We see in Fig. 10, which shows the experimental and estimated damage maps, that if we use this model to estimate the evolution of each individual damage site initiated by the initial laser shot, the computed results compare fairly well with the experimental ones.

5 Discussion–conclusion

The model derived in the previous section has been tested on other data than the one used for its definition. Several configurations have been experimented to study the effect of phase modulations on growth due to amplitude modulations, or the outcome of thickness sample due to non-linear effect as self-focusing. In order to test the quality of the model and to have a quantitative information, we have chosen to compare the percentage of experimentally damaged area with the one predicted by the model. As an example, this model has been applied on the full beam aperture with numerous damage sites, whereas the model and the parameters have been obtained on a reduced area with only few and isolated damage sites. To simulate the growth of all damage sites in the full aperture, the aggregation of different damage sites has to be treated. Two methods have been tested. In the “circle method,” damage sites grow independently and at the end of the sequence, they are superposed. In the “dilate method,” after each shot, two damage sites put together are superposed, gathered in order to obtain only one new damage site that grows independently again. The two methods give very close results, the first one being more rapid. Then a complete

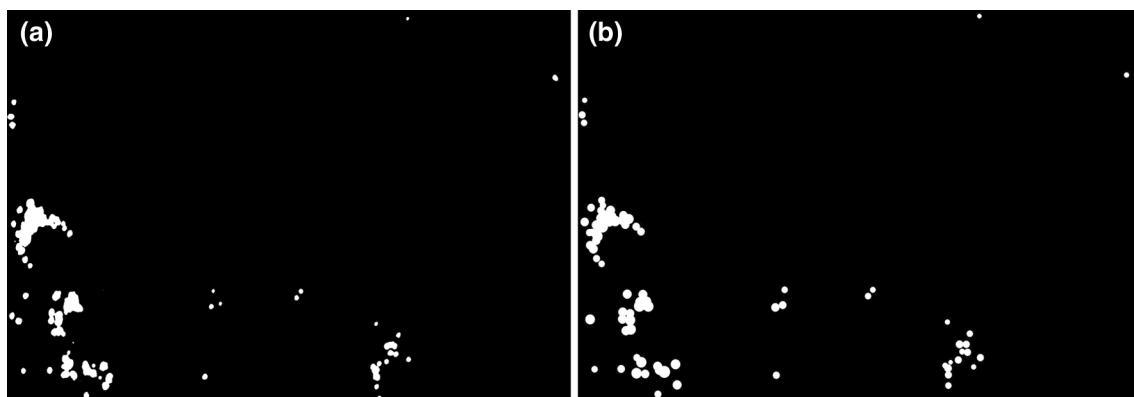


Fig. 10 Subaperture damage map after seven shots. **a** On the left, the experimental map. **b** On the right, the modeling map is obtained using the growth coefficients deduced from the experimental data

growth sequence has been reproduced with the knowledge of fluence maps for each shot and the use of relation (5) to allocate the right growth coefficient of each individual site. Figure 11 exhibits the percentage of damaged area for the entire surface irradiated by the laser for seven successive shots. Damage sites have been initiated at the first shot at higher fluences than the next six shots dedicated to growth. In this graph, bold circles represent the experimental data, whereas bold and empty squares are obtained from the linear and multiparameter models, respectively. It shows together a strong improvement in comparison with the linear model and a good estimation of the experimental results. This is visually confirmed in Fig. 12 which plots the experimental and estimated damage maps. Both maps are quite similar, whereas map obtained from the linear

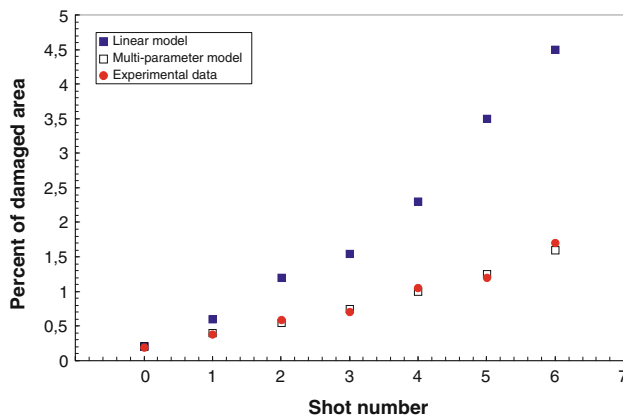


Fig. 11 Damaged area ratio as a function of shot number. The *bold circles* are the experimental data; the *bold squares* are the standard approach (linear model); the *empty squares* represent the results from the modeling approach (multiparameter model)

model exhibits very large damage sites (this is the reason why this map is not reported here, the final picture is too “saturated”). These two figures illustrate the strong improvement with the multiparameter model. This model well reproduces the experiments and allows us to be more predictive, the ultimate goal to determine the lifetime of the optics for a series of shots.

The important progress in this work is the fact to take into account both the mean fluence and the size of the damage shot after shot. The growth coefficient depends mainly on these two parameters and is then adapted to each individual damage and shot. This approach enables us to tackle the uncertainty observed in growth rate even under identical laser conditions. Other issues have been considered such as the damage neighbors and the shot number, but their contributions are less important. It does not mean that there is no effect of laser exposure history, like a “conditioning” effect observed with a fluence ramp [8] which creates small damage sites with lower growth coefficients. In this model the influence of the shot number is closely linked to the damage size. The initial size of damage sites is also an important parameter governing the first steps of the growth.

This study demonstrates that the growth coefficient is size dependent in addition to be fluence dependent. Then a correct description of the growth phenomena has to take into account at least these two parameters. This formalism is now implemented in the algorithm used to optics lifetime prediction for Ligne d’Intégration Laser (LIL) and LMJ facilities. It is important to keep in mind that this statistical approach is well adapted to describe the growth statistically in case of numerous events (damage sites and shots) but is not able to predict the exact size of each damage site shot

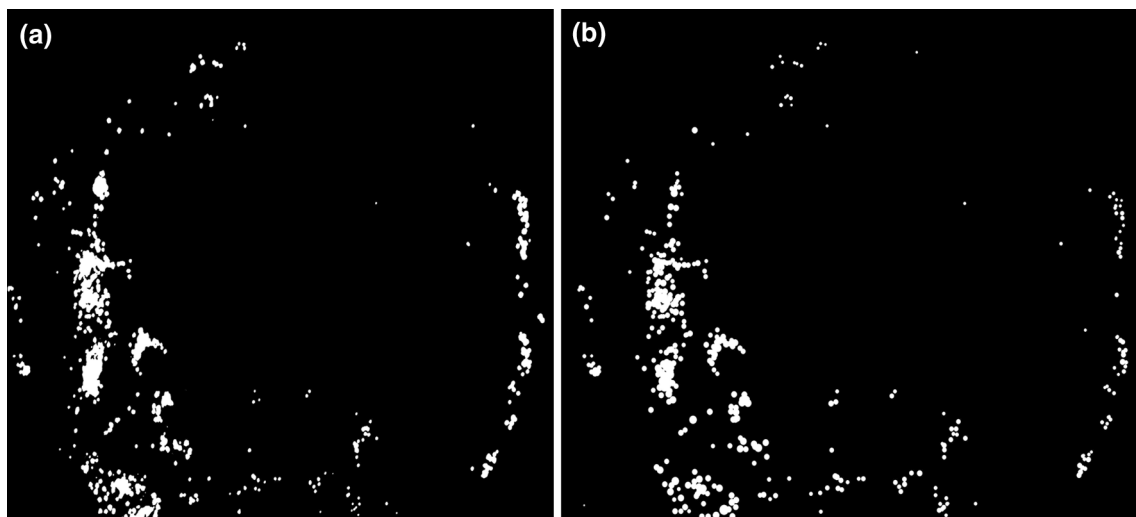


Fig. 12 Full-aperture damage map after seven shots. **a** On the *left*, the experimental full-aperture map. **b** On the *right*, the modeling map is obtained using the growth coefficients deduced from the subaperture map

after shot. This approach is reliable in the fluence range presented in this paper, which corresponds to fluences actually obtained on high-power laser facilities, but it has to be tested at higher fluences corresponding to unwanted spatial modulations. In this approach, damage sites are characterized only by their surface, the total ablated volume and the crack lengths under the damage sites should be carefully measured for a better description of the growth. We now have to precisely study the growth of very large damage sites (few millimeters in diameters), an effect of saturation being suspected. Experiments on large damage sites require the use of very large and homogeneous beams with high repetition rate in order to perform statistical tests. The knowledge of the growth of small and large damage sites will allow a complete description of this phenomenon and will permit a precise prediction of the lifetime optics under operation.

The parametric study taking into account both phase modulations and sample thickness will be presented in a paper dealing with fluence amplification due to nonlinear effect in thick components.

Acknowledgments The authors thank François Dufour and Marie Chavent (Bordeaux Mathematics Institute—IMB) for their fruitful support on statistical methods.

Open Access This article is distributed under the terms of the Creative Commons Attribution License which permits any use, distribution, and reproduction in any medium, provided the original author(s) and the source are credited.

References

1. J. Wong, J.L. Ferriera, E.F. Lindsey, D.L. Haupt, I.D. Hutcheon, J.H. Kinney, Morphology and microstructure in fused silica induced by high fluence ultraviolet 3ω (355 nm) laser pulses. *J. Non-Cryst. Solids* **352**, 255–272 (2006)
2. Z.M. Liao, G.M. Abdulla, R.A. Negres, D.A. Cross, C.W. Carr, Predictive modeling techniques for nanosecond-laser damage growth in fused silica optics. *Opt. Express* **20**, 15569 (2012)
3. M.A. Norton, E.E. Donohue, M.D. Feit, R.P. Hackel, W.G. Hollingsworth, A.M. Rubenchik, M.L. Spaeth, Growth of laser damage on the input surface of SiO_2 at 351 nm. *Proc. SPIE* **6403**, 64030L (2007)
4. M.A. Norton, L.W. Hrubesh, Z. Wu, E.E. Donohue, M.D. Feit, M.R. Kozlowski, D. Milam, P.C. Neeb, W.A. Molander, A.M. Rubenchik, W.D. Sell, P.J. Wegner, Growth of laser initiated damage in fused silica at 351 nm. *Proc. SPIE* **4347**, 468 (2001)
5. H. Bercegol, A. Boscheron, J.M. DiNicola, E. Journot, L. Lemaignère, J. Néauport, G. Razé, Laser damage phenomena relevant to the design and operation of an ICF laser driver. *J. Phys. Conf. Ser.* **112**, 032013 (2008)
6. R.A. Negres, M.A. Norton, D.A. Cross, C.W. Carr, Growth behavior of laser-induced damage on fused silica optics under UV, ns laser irradiation. *Opt. Express* **18**, 19966 (2010)
7. R.A. Negres, Z.M. Liao, G.M. Abdulla, D.A. Cross, M.A. Norton, C.W. Carr, Exploration of the multi-parameter space of nanosecond-laser damage growth in fused silica optics. *Appl. Opt.* **50**, 12 (2011)
8. R.A. Negres, G.M. Abdulla, D.A. Cross, Z.M. Liao, C.W. Carr, Probability of growth of small damage sites on the exit of fused silica optics. *Opt. Express* **20**, 13030 (2012)
9. S.G. Demos, R.N. Raman, R.A. Negres, Time-resolved imaging of processes associated with exit-surface damage growth in fused silica following exposure to nanosecond laser pulses. *Opt. Express* **21**, 4875 (2013)
10. G. Duchateau, M.D. Feit, S.G. Demos, Strong nonlinear growth of energy coupling during laser irradiation of transparent dielectrics and its significance for laser induced damage. *J. Appl. Phys.* **111**, 093106 (2012)
11. L. Lemaignère, G. Dupuy, T. Donval, P. Grua, H. Bercegol, Comparison of laser-induced surface damage density measurements with small and large beams: toward representativeness. *Appl. Opt.* **50**, 441 (2011)
12. L. Lemaignère, M. Balas, R. Courchinoux, T. Donval, J.C. Poncetta, S. Reyné, B. Bertussi, H. Bercegol, Parametric study of laser-induced surface damage density measurements: toward reproducibility. *J. Appl. Phys.* **107**, 023105 (2010)
13. L. Lemaignère, T. Donval, M. Loiseau, J.C. Poncetta, G. Razé, C. Meslin, B. Bertussi, H. Bercegol, Accurate measurements of laser-induced bulk damage density. *Meas. Sci. Technol.* **20**, 095701 (2009)
14. C.W. Carr, M.J. Matthews, J.D. Bude, M.L. Spaeth, The effect of laser pulse duration on laser-induced damage in KDP and SiO_2 . *Proc. SPIE* **6403**, 64030K (2006)
15. T.A. Laurence, J.D. Bude, S. Ly, N. Shen, M.D. Feit, Extracting the distribution of laser damage precursors on fused silica surfaces for 351 nm, 3 ns laser pulses at high fluences (20–150 J/cm²). *Opt. Express* **20**, 11561 (2012)
16. G. Razé, J.M. Morchain, M. Loiseau, L. Lemaignère, M. Josse, H. Bercegol, Parametric study of the growth of damage sites on the rear surface of fused silica windows. *Proc. SPIE* **4932**, 127 (2003)
17. V.M.R. Muggeo, Segmented: an R package to fit regression models with broken-line relationships. *R News* **8/1**, 20 (2008)